Kelvin probe microscopy and electronic transport in graphene on SiC(0001) in the minimum conductivity regime

A. E. Curtin,[1] M. S. Fuhrer,[1,a)] J. L. Tedesco,[2] R. L. Myers-Ward,[2] C. R. Eddy, Jr.,[2] and D. K. Gaskill[2]
[1]*Center for Nanophysics and Advanced Materials, University of Maryland, College Park, Maryland 20742, USA*
[2]*U.S. Naval Research Laboratory, Washington, DC 20375, USA*

(Received 13 December 2010; accepted 2 May 2011; published online 14 June 2011)

Ambient-environment Kelvin probe microscopy of many $(10\ \mu m)^2$ areas of single-layer graphene on SiC(0001) shows area-to-area rms surface potential variation of 12 meV. Electronic transport data are consistent with the minimum conductivity regime. Together the data indicate a highly uniform carrier concentration with a small magnitude ($<10^{12}$ cm^{-2}). We conclude that the previously reported large spread in carrier densities from Hall measurements on similar samples is an artifact of electron–hole puddling in the minimum conductivity regime. © *2011 American Institute of Physics*. [doi:10.1063/1.3595360]

The epitaxial growth of graphene on silicon carbide holds promise for wafer-scale fabrication of this interesting two-dimensional electronic material. Growth on "Si-face" SiC(0001) can produce graphene films of highly uniform thickness, consisting almost exclusively of single-layer graphene (SLG), as evidenced by Raman spectroscopy[1–3] and the half-integer quantum Hall effect unique to SLG.[4–7] However, questions remain as to the electronic uniformity of these films. Understanding the transport properties of the unprocessed samples is a necessary first step in developing an understanding of the properties for processed samples and samples exposed to different ambients. Photoemission,[8,9] STM,[10] and transport[4,5] experiments report a wide range of Fermi energies $+90 \leq E_F \leq +500$ meV relative to the charge neutral point (CNP) for SLG on SiC(0001). A recent transport study[11] of a large number of similar ungated devices, both $(16\ mm)^2$ chips and multiple $(10\ \mu m)^2$ Hall crosses fabricated on the same chip, found large variations in carrier concentrations; electron and hole concentrations exceeding 3×10^{13} cm^{-2} were observed, corresponding to a standard deviation in Fermi energy $E_{F,rms} > 500$ meV.

Here we use Kelvin probe microscopy (KPM) to probe variations in surface potential, and hence Fermi energy, in SLG grown on 6H–SiC (0001). In contrast with the Hall-cross measurements,[11] KPM of widely-spaced $(10\ \mu m)^2$ areas shows an $E_{F,rms}$ of only 12 meV, indicating highly uniform doping on a macroscopic scale. Transport measurements on this sample and many nominally identical samples[11] reveal that the conductivity σ is clustered about a value of $\sim 4e^2/h$, which is consistent with the predicted minimum conductivity for graphene on SiC with a charged-impurity density n_{imp} on order 10^{13} cm^{-2}. This impurity density is also consistent with the mobility on order 1000 cm^2/V s observed for the few highest-conductivity samples with $\sigma \gg 4e^2/h$ which are presumably doped outside the minimum conductivity regime. We conclude that our samples, and the majority of the samples in Ref. 11, are in the low-doped minimum conductivity regime, where the small Hall coefficient was misinterpreted to indicate a high carrier density and large doping variations.

Epitaxial growth of graphene on SiC has been performed in vacuum and argon environments at temperatures ranging from 1150 to 1620 °C.[12–15] These conditions have produced graphene of varying quality with early reports of many-layer graphitic growth on both the Si-face and C-face of SiC. Recently, it has been shown that the use of a inert gas overpressure improves the quality of the graphene, allowing for higher growth temperatures, longer growth times, and producing a larger area percentage of SLG.[16,17] For this experiment, samples were grown on semi-insulating SiC substrates in argon at a pressure of 150 mbar at 1620 °C for 90 min. Extensive Raman mapping of graphene surfaces shows that the majority of the sample surface is monolayer.[1,18]

We performed KPM in ambient conditions using a Co/Cr-coated silicon tip with radius of curvature of ~50 nm. As implemented on the Veeco D5000 scanning probe microscope, the Kelvin probe method uses the lifted tip to perform surface potential measurements interleaved with traditional tapping atomic force microscopy (AFM). The surface potential measurement is performed by applying a 1500 mV ac voltage, $V_{tip,ac}$, to the tip at resonance frequency, ω, with the tip lifted 2–20 nm above the graphene surface and the piezodriver turned off. The tip voltage V_{tip} is controlled by a feedback loop such that the amplitude of the tip at the ac frequency is zero; at this condition $eV_{tip} = W_{tip} - W_{surface}$, where W_{tip} and $W_{surface}$ are the work functions of tip and surface, respectively. For graphene, we expect that $W_{surface} = W_{cnp} - E_F$, where W_{cnp} is the work function of charge-neutral graphene on SiC(0001). Hence V_{tip} directly tracks variation in E_F, and we take the standard deviation in V_{tip} to be equal to $E_{F,rms}/e$.

We performed KPM over seven $(10\ \mu m)^2$ regions of a $(16\ mm)^2$ sample. All the data shown were taken with a single tip over a single session of data collection to eliminate any changes due to ambient doping variation, tip condition, temperature, etc. Figure 1(a) shows topography and Fig. 1(b) surface potential of a single $(10\ \mu m)^2$ scan that was typical of the majority of the sample surface; occasionally a clearly multimodal surface potential distribution was observed.[19] A

a)Electronic mail: mfuhrer@physics.umd.edu.

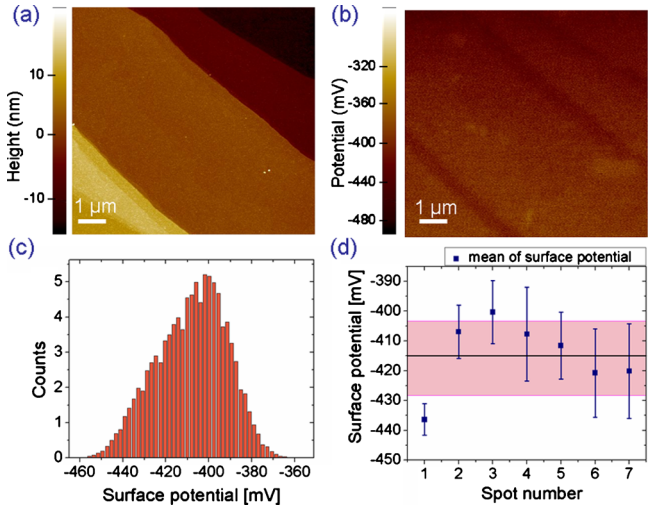

FIG. 1. (Color online) Topography (a) and surface potential (b) collected by KPM on a typical $(10\ \mu m)^2$ region of epitaxial graphene on SiC(0001). (c) Histogram of the potential data from (b). (d) The mean surface potential of seven $(10\ \mu m)^2$ regions and their standard deviation (error bars). The average and standard deviation over all locations are given by the line at 415.2 mV and the shaded box, respectively.

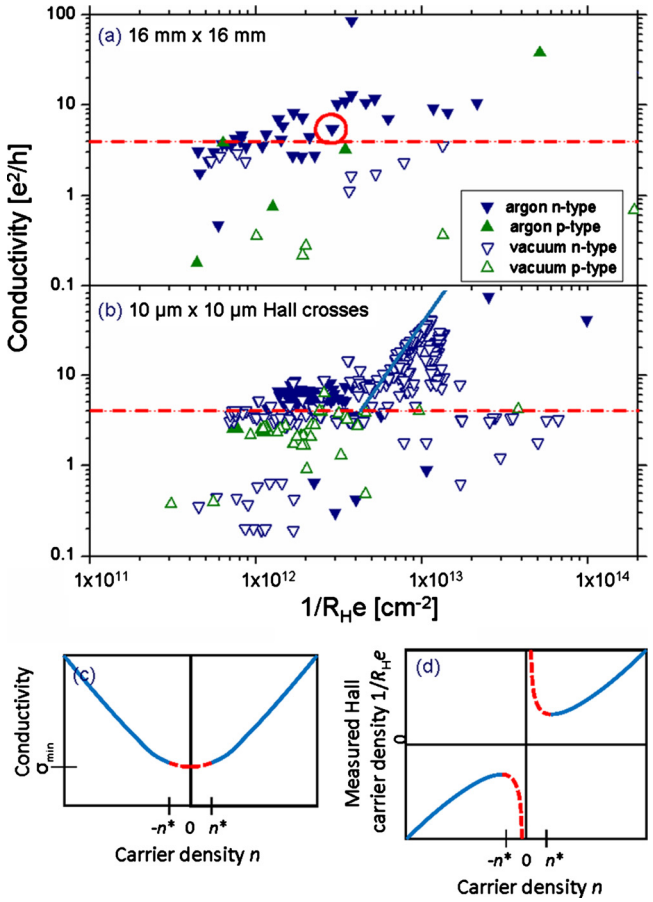

FIG. 2. (Color online) (a) and (b) Conductivity vs apparent Hall carrier density for (a) 16 mm×16 mm van der Pauw samples and (b) 10 μm ×10 μm Hall crosses of epitaxial graphene on SiC(0001), grown in argon (filled symbols) and vacuum (open symbols, Ref. 11). Upward-pointing triangles (green) are p-type and downward-pointing triangles (blue) are n-type. The data point circled in red represents the sample studied in this work. The dashed lines in (a) and (b) are at a conductivity of $3.5e^2/h$. The solid line in (b) is a guide to the eyes, discussed in text. (c) and (d) Conductivity (c) and apparent Hall carrier density $1/R_He$ (d) vs average carrier density, n, within the self-consistent theory of Ref. 22.

histogram of the potential observed over the scanned area is shown in Fig. 1(c). The potential variation over the surface is smooth with no sharp steps correlated with topographical features or otherwise. Figure 1(d) shows the mean and standard deviation of the surface potential for seven widely separated $(10\ \mu m)^2$ scan areas over a 16×16 mm sample. For the data taken at these locations, we found the standard deviation in peak position to be $E_{F,rms}=12$ meV with $E_{F,rms}$ within each individual $(10\ \mu m)^2$ area ranging from 5 to 16 meV.

We occasionally observe multimodal surface potential images with clearly defined regions of different surface potential with boundaries that correspond to topographic steps.[19] We interpret the regions of different surface potential as regions of different graphene layer thickness, e.g., interfacial layer or bilayer graphene (BLG), previously observed to have different surface potentials by Filleter *et al.*[20] The fact that we rarely observe these sharp steps in surface potential suggests that our sample is homogeneous in layer number. However, in Figs. 1(b) and 1(c) there appear to be regions of slightly lower surface potential near step edges. This could indicate the presence of BLG at the step edges, though the potential difference (~25 meV) is much smaller than that observed between SLG and BLG by Filleter *et al.* (~100 meV).[20]

To extract information about the charge carrier concentration variation over the graphene, we relate the peak positions variation plotted in Fig. 1(d) to a variation in E_F, and thus a variation in the carrier density of the sample. Near the CNP, the carrier concentration variation is $\delta n=(E_{F,rms}/\hbar v_F)^2/\pi$, where $v_F=1.1\times10^8$ cm/s is the Fermi velocity in graphene[21] and $\hbar$ is Planck's constant. The macroscopic variation $E_{F,rms}=12$ meV then corresponds to a variation in carrier concentration of $\sim10^{10}$ cm^{-2}. If the sample is highly doped, the carrier concentration variation is approximated by $\delta n=(dn/dE)E_{F,rms}=D(E)E_{F,rms}=2/\hbar v_F\sqrt{n/\pi}E_{F,rms}$, where $D(E)$ is the density of states in graphene. For a doping of $n=10^{13}$ cm^{-2}, the variation $E_{F,rms}=12$ meV would correspond to $\delta n=5\times10^{11}$ cm^{-2}. The variations in carrier density measured by KPM are therefore much smaller than the apparent variations measured by Hall resistivity.

To address this discrepancy, we re-examine the transport data in Ref. 11. Figures 2(a) and 2(b) show transport data from nominally identical samples prepared in argon, as well as from samples grown in vacuum and reported in Ref. 11, replotted as sheet conductivity versus apparent Hall carrier density $1/R_He$, where R_H is the Hall coefficient of each sample. The conductivity is seen to cluster around a value of $\sim4e^2/h$ over a wide range of carrier densities, with the exception of the vacuum-grown 10 μm Hall crosses [Fig. 2(b)] where for an intermediate carrier density range of $0.5-1.5\times10^{13}$ cm^{-2}, there is a cluster of points whose conductivities rise rapidly with carrier density. The data point circled in red in Fig. 2(a) corresponds to the sample in this study (imaged in Fig. 1), which has a conductivity of $5.3e^2/h$ and an apparent Hall carrier density of 2.8×10^{12} cm^{-2}.

We interpret the data in Figs. 2(a) and 2(b) within the self-consistent Boltzmann theory for graphene dominated by charged impurities put forth by Adam *et al.*[22] Figures 2(c) and 2(d) show qualitatively how σ and $1/R_He$ are expected

to vary with average carrier density, n. At high n (solid blue lines), the conductivity is proportional to n (constant mobility) and the apparent Hall carrier density $1/R_H e$ asymptotically approaches the average carrier density n. For $n < n^*$, graphene is dominated by electron and hole puddles with an rms carrier density n^* caused by the random charged impurity potential (red dashed lines). The conductivity is roughly constant around a minimum value σ_{min} of a few e^2/h, and the apparent Hall carrier density diverges as $n \to 0$. The apparent Hall carrier density always overestimates the average carrier density n, and is never less than $\sim n^*$.

In Fig. 2(b) the highest conductivity devices have $\sigma \approx 50e^2/h$. We assume that these devices are in the high-density regime, and $n \approx 1/R_H e \approx 10^{13}$ cm^{-2}, indicating a mobility $\mu \approx 1000$ cm^2/V s. Applying the self-consistent theory of Adam *et al.*[22] to the case of graphene on SiC ($\kappa \approx 9.6$), this corresponds to a charged impurity density of $n_{imp} \approx 8 \times 10^{12}$ cm^{-2}, $n^* \approx 8 \times 10^{11}$ cm^{-2}, and $\sigma_{min} \approx 3.5e^2/h$. We observe a large number of samples ($\sim$50% of vacuum-grown, and nearly all argon-grown samples) with conductivities $\sim 3.5e^2/h$, and $1/R_H e > 7 \times 10^{11}$ cm$^{-2} \approx n^*$; and we conclude that these samples are in the low density minimum conductivity regime $n < n^* \approx 8 \times 10^{11}$ cm^{-2}. This indicates that our SLG on SiC(0001) in ambient has much lower doping than has been previously reported.

The very small spread in surface potential measured by KPM indicates a uniform doping level on a macroscopic scale. The transport data are inconsistent with a uniform *high* doping level $n > n^*$: in this case one would expect all the samples to be outside the minimum conductivity regime, and display high conductivity and a narrowly distributed Hall carrier density which reflects the true carrier density. We conclude that the samples as probed by KPM are uniformly doped in the minimum conductivity regime $|n| < n^* \approx 8 \times 10^{11}$ cm^{-2}. We further conclude that the previously reported[11] large spread in carrier densities from Hall measurements on similar samples is an artifact of electron–hole puddling in the minimum conductivity regime.

Our conclusion is consistent with top-gated field-effect transistors fabricated on similar SLG on SiC(0001) showing low threshold voltages.[23] The microscopic fluctuations within a single surface potential image, $E_{F,rms} = 5-16$ meV are approximately one order of magnitude smaller than the electron–hole puddle fluctuations $E_{F,rms} = 110$ meV for $n^* \approx 8 \times 10^{11}$ cm^{-2}. We assume that the discrepancy results from the puddle correlation length of 10–20 nm being an order of magnitude smaller than the resolution of the Kelvin probe measurement. It is not clear why previous experiments[4,8,9,11] on SLG on SiC(0001) show much higher doping. In Ref. 11, high doping was inferred incorrectly from Hall measurements in the minimum conductivity regime, but ARPES (Refs. 8 and 9) and some transport measurements performed in vacuum[4] clearly show highly and uniformly doped SLG ($n \approx 10^{13}$ cm^{-2}). We infer that exposure to ambient causes compensating p-doping or passivation of samples that were highly n-doped as-grown in vacuum.

J.L.T. is grateful to the ASEE for postdoctoral fellowship support. Work at NRL was supported by the Office of Naval Research. A.E.C. and M.S.F. acknowledge support from the University of Maryland NSF-MRSEC and MRSEC shared facilities under Grant No. DMR 05-20741.

[1] J. A. Robinson, M. Wetherington, J. L. Tedesco, P. M. Campbell, X. Weng, J. Stitt, M. A. Fanton, E. Frantz, D. Snyder, B. L. VanMil, G. G. Jernigan, R. L. Myers-Ward, C. R. Eddy, and D. K. Gaskill, Nano Lett. **9**, 2873 (2009).
[2] Z. H. Ni, W. Chen, X. F. Fan, J. L. Kuo, T. Yu, A. T. S. Wee, and Z. X. Shen, Phys. Rev. B **77**, 115416 (2008).
[3] C. Faugeras, A. Nerriere, and M. Potemski, Appl. Phys. Lett. **92**, 011914 (2008).
[4] J. Jobst, D. Waldmann, F. Speck, R. Hirner, D. K. Maude, T. Seyller, and H. B. Weber, Phys. Rev. B **81**, 195434 (2010).
[5] A. Tzalenchuk, S. Lara-Avila, A. Kalaboukhov, S. Paolillo, M. Syväjärvi, R. Yakimova, O. Kazakova, T. J. B. M. Janssen, V. Fal'ko, S. Kubatkin, Nat. Nanotechnol. **5**, 186 (2010).
[6] X. Wu, Y. Hu, M. Ruan, N. K. Madiomanana, J. Hankinson, M. Sprinkle, C. Berger, and W. A. de Heer, Appl. Phys. Lett. **95**, 223108 (2009).
[7] T. Shen, J. J. Gu, M. Xu, Y. Q. Wu, M. L. Bolen, M. A. Capano, L. W. Engel, and P. D. Ye, Appl. Phys. Lett. **95**, 172105 (2009).
[8] A. Bostwick, T. Ohta, T. Seyller, K. Horn, and E. Rotenberg, Nat. Phys. **3**, 36 (2007).
[9] T. Ohta, A. Bostwick, J. L. McChesney, T. Seyller, K. Horn, and E. Rotenberg, Phys. Rev. Lett. **98**, 206802 (2007).
[10] G. M. Rutter, N. P. Guisinger, J. N. Crain, E. A. A. Jarvis, M. D. Stiles, T. Li, P. N. First, and J. A. Stroscio, Phys. Rev. B **76**, 235416 (2007).
[11] J. L. Tedesco, B. L. VanMil, R. L. Myers-Ward, J. M. McCrate, S. A. Kitt, P. M. Campbell, G. G. Jernigan, J. C. Culbertson, C. R. Eddy, and D. K. Gaskill, Appl. Phys. Lett. **95**, 122102 (2009).
[12] K. V. Emtsev, T. Seyller, F. Speck, L. Ley, P. Stojanov, J. D. Riley, and R. G. C. Leckey, in Sixth European Conference on Silicon Carbide and Related Materials, ECSCRM, Newcastle Upon Tyne, UK, Sept. 3rd-7th, 2006.
[13] T. Ohta, F. El Gabaly, A. Bostwick, J. L. McChesney, K. V. Emtsev, A. K. Schmid, T. Seyller, K. Horn, and E. Rotenberg, New J. Phys. **10**, 023034 (2008).
[14] P. N. First, W. A. de Heer, T. Seyller, C. Berger, J. A. Stroscio, and J.-S. Moon, MRS Bull. **35**, 296 (2010).
[15] E. Rollings, G.-H. Gweon, S. Y. Zhou, B. S. Mun, J. L. McChesney, B. S. Hussain, A. V. Fedorov, P. N. First, W. A. de Heer, and A. Lanzara, J. Phys. Chem. Solids **67**, 2172 (2006).
[16] J. L. Tedesco, B. VanMil, R. L. Myers-Ward, J. Culbertson, G. Jernigan, P. Campbell, J. M. McCrate, S. A. Kitt, C. Eddy, Jr., and D. K. Gaskill, *ECS Transactions* (ECS, San Francisco, CA, 2009), pp. 137–150.
[17] K. V. Emtsev, A. Bostwick, K. Horn, J. Jobst, G. L. Kellogg, L. Ley, J. L. McChesney, T. Ohta, S. A. Reshanov, J. Rohrl, E. Rotenberg, A. K. Schmid, D. Waldmann, H. B. Weber, and T. Seyller, Nature Mater. **8**, 203 (2009).
[18] N. Ferralis, R. Maboudian and C. Carraro, Phys. Rev. Lett. **101**, 156801 (2008).
[19] See supplementary material at http://dx.doi.org/10.1063/1.3595360 for AFM topography and KPM potential images of graphene on SiC showing a multimodal potential distribution.
[20] T. Filleter, K. V. Emtsev, T. Seyller, and R. Bennewitz, Appl. Phys. Lett. **93**, 133117 (2008).
[21] K. S. Novoselov, A. K. Geim, S. V. Morozov, D. Jiang, M. I. Katsnelson, I. V. Grigorieva, S. V. Dubonos, and A. A. Firsov, Nature (London) **438**, 197 (2005).
[22] S. Adam, E. H. Hwang, V. M. Galitski, and S. Das Sarma, Proc. Natl. Acad. Sci. U.S.A. **104**, 18392 (2007).
[23] C. Dimitrakopoulos, Y.-M. Lin, A. Grill, D. B. Farmer, M. Freitag, Y. Sun, S.-J. Han, Z. Chen, K. A. Jenkins, Y. Zhu, Z. Liu, T. J. McArdle, J. A. Ott, R. Wisnieff, and P. Avouris, J. Vac. Sci. Technol. B **28**, 985 (2010).